Catena 208 (2022) 105731

Contents lists available at ScienceDirect

Catena

journal homepage: www.elsevier.com/locate/catena

Processes of neck cutoff and channel adjustment affected by seeding herbaceous vegetation and variable discharges

Zhiwei Li [a], Peng Gao [b,*], Xinyu Wu [c]

[a] State Key Laboratory of Water Resources and Hydropower Engineering Science, Wuhan University, Wuhan 430072, China
[b] Department of Geography and the Environment, Syracuse University, Syracuse, NY 13244, USA
[c] School of Hydraulic Engineering, Changsha University of Science & Technology, Changsha 410114, China

ARTICLE INFO

Keywords:
Neck cutoff
Riparian vegetation
Bank erosion
Variable discharges
Meandering channel
Flume experiment

ABSTRACT

The goal of this study is to quantify morphodynamic roles of riparian vegetation and variable discharges in the process of neck cutoff, which is difficult to determine in natural meandering rivers due to the prolonged process and unpredictable occurrence of neck cutoffs. We achieved the goal in a highly sinuous flume channel (25 m × 6 m × 0.4 m) that has a mobile bed and includes seven bends with the narrowest neck of 0.22 m. Its banks and floodplain were covered by dense herbaceous vegetation (i.e., *Festuca elata*) seeded 10 days before each of three experiments that had different vegetation density and discharge arrangements. They are the first set of experiments of achieving neck cutoffs in a laboratory flume channel with vegetation. We examined temporal changes of the narrowest neck width and planform of the bend that had neck cutoff, measured temporal changes of the mean channel width and its final width/depth ratio, and tracked the temporal changes of their mean slopes and width/depth ratio. Our results revealed that (1) herbaceous vegetation can significantly extend the period of neck narrowing process such that neck cutoff may still take a long time even after neck width is about 0.4 of the mean channel width; (2) higher variable discharges only have limited impact on shortening this period; (3) neck cutoff is triggered by seepage flow that is incapable of generating sediment pulses and thus the morphological adjustment of the upstream and downstream reaches are mainly caused by changes of channel hydraulics rather than sediment deposition as in the case of chute cutoff. Our experiments show a new way of replicating neck cutoff in flume experiments and our findings provide new insight into understanding processes of neck cutoff in natural highly sinuous meandering rivers.

1. Introduction

Neck cutoff is an indispensable geomorphic event in the long-term morphodynamic process and an adjuster of the periodic self-evolution of meandering rivers (Camporeale et al., 2008; Güneralp and Marston, 2012; Hooke, 2013; Ondruch et al., 2018; Seminara, 2006; Stølum, 1996). It occurs when the upper and lower channel on both sides of the neck is connected after the neck width in a typical Ω-shaped bend is continuously shortened by bank erosion and collapse (Constantine and Dunne, 2008; Erskine et al., 1992; Gay et al., 1998; Li et al., 2019; Schwenk et al., 2015). Possible modes of triggering neck cutoff include: (i) medium to high flow eroding and cutting through the neck, and (ii) progressive bank erosion and intermittent bank collapse interconnecting the neck. Except man-made causes inducing neck cutoff (Coomes et al., 2009; Li and Gao, 2019; Pan et al., 1978; Winkley, 1977), the first mode often occurs in a relatively short duration (several days or weeks) because of extremely high erosion intensity, while the second may last longer before connection of the upstream and downstream channel due to relatively low erosion rates resulted from inhibition of riparian vegetation and high resistance of cohesive soils (Braudrick et al., 2009; Schwendel et al., 2015). Therefore, unraveling occurrence, process, and threshold conditions of neck cutoff requires distinguishing the difference between the two modes.

The first mode can be triggered by low-frequency, but high-magnitude floods. Combining with a higher local gradient between the upper and lower part of the neck, this flow is sufficiently powerful to erode the floodplain and finally link the upstream and downstream channels even though the floodplain is generally protected by riparian vegetation cover (e.g., grasses, shrubs, trees) and cohesive soils. This mode has been widely reported for rivers in the North American Plain,

* Corresponding author.
E-mail address: pegao@maxwell.syr.edu (P. Gao).

https://doi.org/10.1016/j.catena.2021.105731
Received 7 March 2021; Received in revised form 8 August 2021; Accepted 11 September 2021
Available online 20 September 2021

Amazon River basin, Great Britain, and China (i.e., Yangtze, Weihe, and Tarim Rivers) (Erskine et al., 1992; Fares, 2000; Gay et al., 1998; Hooke, 1995, 2004; Li et al., 2017; Liu et al., 2017; Pan et al., 1978). River bends with reported first mode of neck cutoff were generally within large river reaches and occurrence of neck cutoff was caused by extreme flood events that may produce relatively higher flows for initiating headward erosion. Its mechanisms, which are caused by large discharges, are well known, but its occurrence is rarely observed (Erskine et al., 1992; Hooke, 1995).

The second mode generally occurs in vegetated bends with low and medium water discharges where bank erosion and collapse progressively shorten neck width until the pressure derived from the local difference of water level on two sides of the neck is large enough to break the neck. This mode, which is often constrained by the inhibition effect of riparian vegetation and clay material on river banks, has been commonly found in rivers within Australia, northern British, South America, and Qinghai-Tibet Plateau (Erskine et al., 1992; Hooke, 1995; Schwendel et al., 2015; Schwenk and Foufoula-Georgiou, 2016). Based on these studies, the processes of the second mode can be generalized in three stages: (i) the neck width of a typical Ω-shaped bend is narrowed by continuous bank erosion and collapse, such that it becomes less than the average channel width; (ii) water level difference between upstream and downstream neck gradually builds up a seepage pressure in neck; (iii) the neck is broken which is followed by prompt expansion of a new cutoff channel. Although we realized that Hooke (1995) had observed and analyzed historical sequences of a neck cutoff in No. 1 bend of River Bollin using field survey before and after this cutoff occurred, the triggering mechanism of neck cutoff still awaits validation using more detailed data collected from natural meandering rivers.

Thus far, very few *in situ* measurements on the processes of neck cutoff are obtained from natural meandering rivers as its occurrence is almost impossible to capture directly due to uncertainty and short duration of a cutoff incident. Accordingly, little is available for validating these processes, though its counterpart, chute cutoff has been widely studied using field observations, historical maps, and remote sensing imagery (Eekhout and Hoitink, 2015; Erskine et al., 1992; Hooke, 1995; Lewis and Lewin, 1983; Lonsdale and Hollister, 1979; Richards and Konsoer, 2020; Schwenk and Foufoula-Georgiou, 2016; Słowik, 2016; van Dijk et al., 2014; Viero et al., 2018; Zinger et al., 2011, 2013), as well as flume experiments (Braudrick et al., 2009; van Dijk et al., 2012; Yin, 1965).

What remains possible is using laboratory flumes to reproduce processes controlling neck cutoff. Yet, the complex interaction among flow, sediment, and vegetation makes it very difficult to reproduce these natural processes in flume experiments. The biggest challenge is how to effectively constrain the often over-expansion of channel width so that the meandering channel may continuously evolve as in real rivers. Naturally planting vegetation in laboratory flumes is a logic means of solving this problem, because riparian vegetation grown on banks of most alluvial rivers plays a vital role in development, evolution, and stability of small and medium scale meandering rivers (Camporeale et al., 2013; Camporeale and Ridolfi, 2010; Goodson et al., 2016; Hopkinson and Wynn, 2009; Li et al., 2016; Perucca et al., 2007; Pollen-Bankhead and Simon, 2010; van Dijk et al., 2013). Many studies have shown that the upper layer of river bank forms the soil-root composite, in which vegetation stems and leaves are laterally attached to the bank and inserting into the near-bank flow (Tal and Paola, 2010; van Dijk et al., 2013). This composite improves erosion resistance of the upper soil and inhibits lateral erosion rate up to an order of magnitude (Ielpi and Lapotre, 2020; Krzeminska et al., 2019; Midgley et al., 2012; Zhu et al., 2020). Moreover, vegetation stems and leaves may disturb the near-bank flow, increase flow roughness, and reduce erosion capability (Goodson et al., 2016; Hopkinson and Wynn, 2009; Krzeminska et al., 2019; Nepf, 2012). Consequently, riparian vegetation can enhance the stability of river banks, facilitate formation of narrow and deep meandering channels, decrease near-bank flow velocity, which may subsequently improve the resistance of bank erosion, and inhibit the rate of bank collapse (Camporeale et al., 2013; Crosato and Saleh, 2011; Dehsorkhi et al., 2010; Edmaier et al., 2011; Krzeminska et al., 2019; Kyuka et al., 2021; Oorschot et al., 2016; Tal and Paola, 2010; van Dijk et al., 2013; Yang et al., 2018). Surprisingly, growing real vegetation in experimental meandering channels was only occasionally achieved for chute cutoff (Braudrick et al., 2009). Hitherto, neck cutoff has not been successfully replicated in any flume experiment, though it was achieved in a small sand table without vegetation (Han et al., 2015). Clearly, planting vegetation in laboratory flumes has caused a dilemma in the current design for replicating neck cutoff. On the one hand, vegetation stabilizes channel banks, allowing a meandering channel to develop. On the other hand, it significantly reduces migration rate, such that the chance of a neck cutoff incident becomes slim.

To overcome this dilemma, we developed a different approach (Li et al., 2019). Instead of letting an initial straight or less sinuous channel to migrate freely, we manually created a highly convoluted meandering channel that includes an Ω-shaped bend with the length of its neck (L_n) less than the mean channel width (W). With input discharge far lower than the bankfull discharge and without vegetation cover, we were able to achieve neck cutoff in a wide laboratory flume (Li et al., 2019). Essentially, this approach skips the prolonged bend narrowing process, which may take decades or even centuries in natural rivers, and focuses on the crucial stage when $L_n < W$ and neck cutoff is an inevitable outcome. It requires that the initially created channel in the flume geometrically reflects the prototype of real meanders. In this study, the prototypes are many meandering rivers in the Upper Yellow River region including Maduo-Dari, Zoige, Gannan, and Huangnan sub-regions that are covered by grass, meadow, or peat (Gao et al., 2021; Li et al., 2016; Li and Gao, 2019; Wang et al., 2016; Zhu et al., 2020). Many of them (e.g., Black, White, Lanmucuo, and Zequ Rivers) include highly sinuous reaches featured by ample Ω-shaped bends whose neck has a length much less than the mean channel width (Guo et al., 2019).

Although our previous experiments successfully triggered neck cutoff with constant discharges, they missed two important factors affecting the process of neck cutoff: (1) riparian vegetation; and (2) variable discharges. This study aims at filling this gap by growing local herbaceous grass along the banks and floodplain of the created meandering channel with high sinuosity in the same flume and performing three runs with different sets of input discharges. We first reported detailed process of neck cutoff in these experiments. Then, we showed morphodynamic response of the channels to neck cutoff. Finally, we developed an empirical model that quantifies the evolution processes of neck cutoff.

2. Methods

2.1. Flume setup and riparian vegetation selection

Experiments for neck cutoff were conducted in a laboratory flume that has been described earlier in detail (Li et al., 2019) and hence only summarized here briefly. The flume is 25 m long, 6 m wide, and 0.4 m deep with a mobile bed (Fig. 1a). A trapezoid-shaped head tank with a short edge, long edge, width, and depth of 2.2, 6.0, 2.2, and 0.6 m, respectively, is connected to a rectangular pool of 1.8 m long, 6.0 m wide, and 0.4 m deep for achieving steady flow at the flume inlet (Fig. 1a). The input discharge is controlled by a pump and measured by an electromagnetic flow meter with an accuracy of 0.001 m^3/h. The flume outlet is connected to a sediment settling pool of 2 m long and a tail water pool of 1.5 m long equipped with a tailgate at the center (Fig. 1a). A loose layer on the bed with a thickness of 0.2 m consists of non-cohesive quartz sand with a median size, $d_{50} = 0.327$ mm. Within the flume, a highly sinuous meandering channel was manually created to reflect planform structure of meanders with high sinuosity in the Zoige basin, located on the northeastern side of Qinghai-Tibet Plateau, China. Process of each experimental run was recorded by six video cameras of 4 million pixels above the center of the flume. The channel

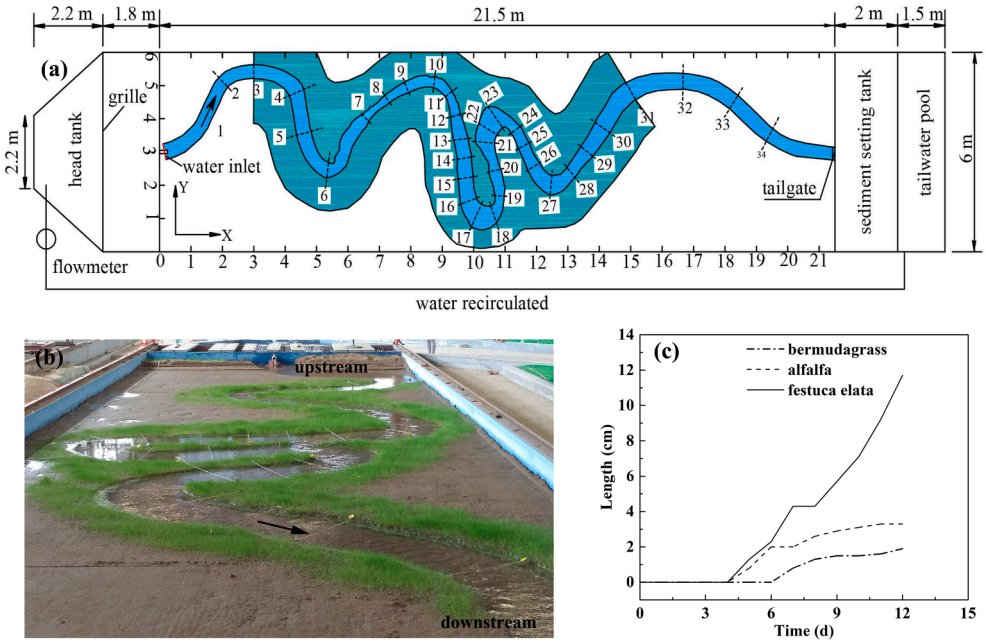

Fig. 1. Sketch of the laboratory flume. (a) Design of the flume. The shaded area represents the section covered by vegetation. (b) An example of matured riparian grass during experiments (c) Comparison of growing processes of the three vegetation selected species.

created before each run included 7 bends, four of which (bend 3 to 6) formed the experimental section containing cross sections from number S7 to S30 (Fig. 1a). This section was divided into three components, which were the upstream (i.e., S7-S13), neck (i.e., S13-S21), and downstream (i.e., S21-S30) reaches. S11, S19, and S24 were the representative cross sections in the three reaches. It should be noted that after neck cutoff, the neck reach becomes the oxbow reach. Riparian vegetation was reflected by growing grass along the banks and floodplains between bends (Fig. 1b).

Riparian vegetation in flume experiments has been commonly represented by growing along banks of flume channels alfalfa sprout (Braudrick et al., 2009; Gran and Paola, 2001; Kyuka et al., 2021; Tal and Paola, 2007, 2010; van Dijk et al, 2013), rice stem (Dehsorkhi et al., 2010), or *Agrostis stolonifera* (Yang et al., 2018). However, the laboratory holding our flume is located in central China that has humid and hot summer, but relatively mild and dry winter. Therefore, these herbaceous species may not be the most appropriate choice for representing riparian vegetation under the local weather and laboratory conditions (e.g., temperature, moisture, and light). Prior to experiments, we systematically tested three species including *Bermudagrass*, *Medicago Sativa* (alfalfa sprout), and *Festuca elata* for identifying the most suitable one for representing riparian vegetation in our flume. *Bermudagrass* is a low-lying herb that may grow quickly. The average growth rate of its stem is 0.0091 m/day. At its mature stage, *Bermudagrass* has the stem that may be 0.1–0.3 m high, and 0.0001–0.00015 m in diameter. The mature alfalfa sprout is typically 0.3–0.9 m high. *Festuca elata* tends to grow solitarily in nature, typically having a height of 0.9–1.2 m and a median diameter of 0.0002–0.00025 m. Our tests involved in growing their seeds in three different base materials (i.e., soil, soil-sand, and sand) and measuring their growth length over three months. Among the three species, *Festuca elata* had the highest growth rates (Fig. 1c). Although it started to germinate after about 4.5 days, similar to that of the other two species, its growth rate was much higher than that in the other two species and this difference of rates increased with time. Thus, for the same time period and similar soil conditions, *Festuca elata* could grow much faster than *Bermudagrass* and *alfalfa sprout*. For example, the stem length of *Festuca elata* reached 0.01 m high in 5 days, but 0.1 m in 10 days after germination and the root length could be more than 0.06 m. Furthermore, *Festuca elata* had high germination rate (70% of 1.0×10^{-4} m^2), and developed a thin and soft root system within a sand bed with a wet riparian condition. The role of planted vegetation here is mainly reflected in the stem of 2.0–2.5 mm diameter, and the role of root can be ignored because the root diameter is only 0.1–0.3 mm. It could also survive for a longer time period (more than three months). Consequently, *Festuca elata* was selected as riparian vegetation around the meandering channel in our flume experiments. Similar to previous flume experiments (Braudrick et al., 2009; van Dijk et al, 2013), the role of vegetation on resistance to bank erosion is mainly embodied in increasing hydraulic resistance through the stems hanging over the bank (Fig. 1b). It is not directly scalable to the real river size as the channel depths in the flume are too small to accurately represent the true vertical structure of a real river bank. Yet, the hydraulic effect of vegetation on bank erosion is comparable to that in real rivers.

2.2. Experiment design and measurement

Three experiments (i.e., RUN 8, 9, and 10) were performed. Each run began with the same geometric configuration of an initial channel, characterized by a mean channel slope of 1.7‰ and a mean width/depth ratio of 4.38 with the depths varying between 0.38 and 0.45 m. Neck cutoff is expected to occur near the neck of bend 4 that had the shortest width of 0.22 m, but was not always the case. Development of neck cutoff refers to the duration from the beginning of an experiment to the moment when the intersection of the neck upstream–downstream channel occurred. The ratio of the initial neck width to the average channel width was typically about 0.4.

After creating the initial meandering channel, *Festuca elata* was manually seeded along banks and floodplain of the experimental section (i.e., from S3 to S31) (Fig. 1a) and watered daily for 10 days. Once germinated (typically in 3–5 days), grass across the growing section (Fig. 1b) was randomly sampled for measuring root and stem lengths and five sites were chosen for determining the mean grass density each day. Although the grass in all three runs covered a similar extent (i.e., S3-S31) and area of 38.46 m^2, its growing pattern was different (Fig. 2), possibly because of different air temperature and moisture during experiments, which lasted from May to August in 2018.

Grass root and stem grew synchronously, but the growth rate varied between them. In the first 10 days, RUN 9 had a higher initial growth

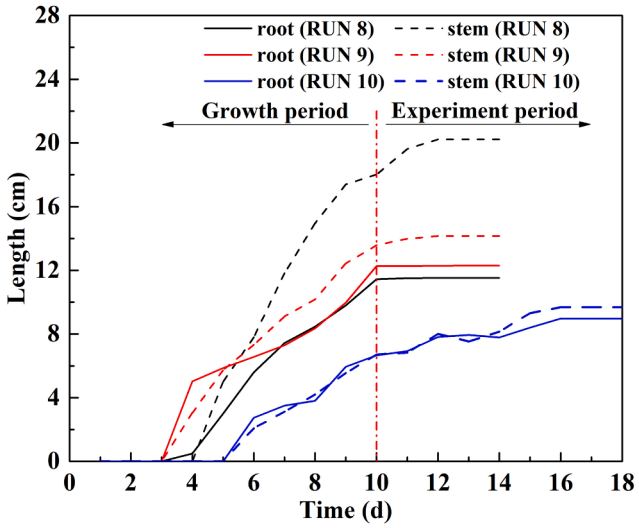

Fig. 2. Growth of root and stem of *Festuca elata* after germination. The vertical dashed line denotes the commencement of the experiments (i.e., the 10th day).

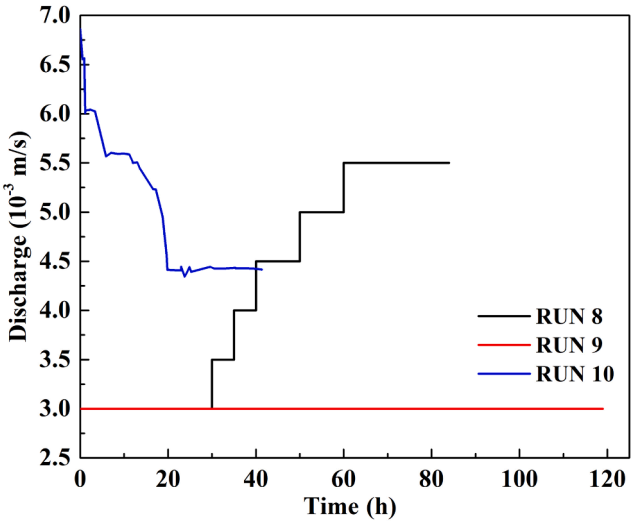

Fig. 3. Temporal patterns of input discharges in RUN 8, 9, and 10.

rate than RUN 8 and quickly adjusted the rate similar to that in RUN 8 (Fig. 2), leading to a greater root length in RUN 9 (i.e., 0.1229 m) than in RUN 8 (i.e., 0.1153 m) (Table 1). The growth rate in RUN 10 was discernibly lower than that in the other two, giving rise to a shorter root length at the 10th day (i.e., 0.0898 m). After this day, the root in RUN 8 and 9 stopped growing, while in RUN 10 remained growing, but with a lower rate. Thus, the root length was always smaller than that in the other two at the end of experiments (Fig. 2). The grass stem was generally longer than the root with the difference, highest in RUN 8 (43%), medium in RUN 9 (13.1%), and lowest in RUN 10 (7.3%) (Table 1). The growth rate of stem followed the same order and the stem continued to grow after the 10th day, though at much lower rates (Fig. 2). The mean grass density based on 31 samples over the entire experimental period decreased in the order of RUN 8, 9, and 10, but the highest one (i.e., 6.8×10^{-3} per m^2) was only about 25% denser than the lowest one (i.e., 5.1×10^{-3} per m^2) (Table 1). Overall, the effect of riparian vegetation is the greatest in RUN 8, the least in RUN 10.

Three runs (RUN 8, 9, and 10) were designed to represent different hydrologic and riparian vegetation conditions (Table 1). RUN 8 had input discharges varied from 3 to 5.5×10^{-3} m^3/s (Fig. 3). The initial input discharges lasted for 30 h and was increased to 3.5×10^{-3} m^3/s for 5 h after measuring the topography of representative cross sections. It was subsequently increased by 5×10^{-4} m^3/s every 5 h till 4.0×10^{-3} m^3/s and then every 10 h till 5.5×10^{-3} m^3/s for attempt of triggering neck cutoff. After 70 h without cutoff, though the input discharge was relatively high (the mean water level was about 0.32 m), RUN 8 entered the second phase, in which grass stem was trimmed from the bed surface using a clipper to encourage bank erosion around the neck and the same input discharge (i.e., 5.5×10^{-3} m^3/s) lasted till the end of experiment at the 84.08th hour (Table 1). During this run, water level along the channel was measured every 6 h for determining channel slopes in the three reaches, and profiles of S11, S12, S13, S19, S21, S22, S24, and S28 were measured at the 30th, 60th, 70th, 72.08th, and 84th hour, respectively.

The input discharge of RUN 9 was set as a constant of 3.0×10^{-3} m^3/s with the mean water level of 0.29 m (Fig. 3) such that the experimental results may be compared with those in RUN 5 that had no vegetation cover and were reported in our earlier study (Li et al., 2019). Similar to RUN 8, neck cutoff did not happen in the first 70 h and thus grass stem covering the banks around the neck was trimmed to facilitate neck cutoff. The second phase of RUN 9 ended at the 119.06th hour (Table 1). During this run, the water level and water depth in the three reaches were measured every 6 h, while the profiles of S11, S12, S13, S19, S21, S22, S24, and S28 were measured every 12 h.

RUN 10 involved a series of variable input discharges decreasing from 6.7 to 4.5×10^{-3} m^3/s in the end with the initial water level of 0.31 m (Fig. 3). They were selected to achieve near bankfull stages without causing overbank flow during the experiment. Discharges were decreased consecutively to replicate the flow regime derived from the falling limb of a hydrograph. In this experiment, neck cutoff occurred without cutting the grass stem and similar measurements were performed.

3. Results and analyses

3.1. Processes of neck cutoff

3.1.1. Neck width

Temporal changes of the neck width (W_n) were different in the three runs, showing their different pathways of developing neck cutoff. In RUN 8 with variable discharges, the reduction rate (R_w) of neck width experienced several different periods (Fig. 4). In the first period (i.e., 0–11 h), it was 0.011 m/h, causing W_n decreased from the original 0.461 to 0.355 m. In the next (i.e., 11–17 h) period, $R_w = 0$ and W_n remained unchanged. The following period of the 17–30 h was featured by a similar R_w (i.e., 0.009 m/h) with W_n quickly decreased to 0.241 m (Table 2). These changes happened under the same input discharge (i.e., $Q = 3$ m^3/s) (Fig. 3), reflecting the initial adjustment of channel morphology. Increase of Q to 3.5 m^3/s in the period of 30–35 h only led

Table 1
Initial and boundary conditions of three designed runs.

No.	Discharge ($\times 10^{-3}$ m^3/s)	Mean root length ($\times 10^{-2}$ m)	Mean stem length ($\times 10^{-2}$ m)	Grass density ($\times 10^{-2}$ m^2)	Days of grass growth before running experiment (days)	Duration (hours)
RUN 8	3.0–5.5	11.53	20.23	0.68	10	84.08
RUN 9	3.0	12.29	14.15	0.55	10	119.06
RUN 10	~bankfull	8.98	9.69	0.51	10	41.33

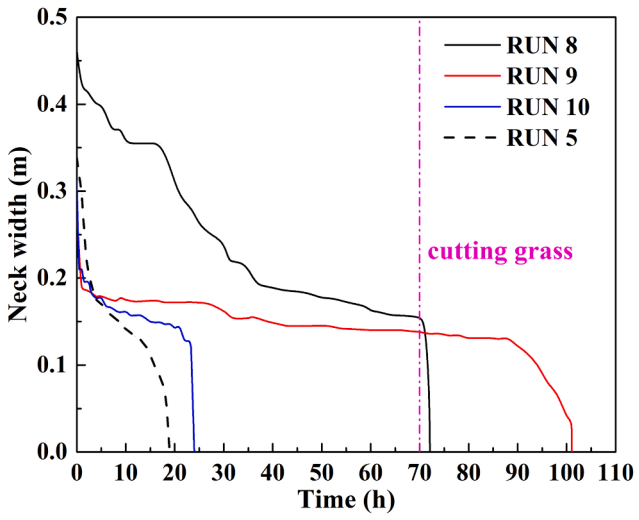

Fig. 4. Temporal changes of neck width in RUN 8, 9, and 10. The red curve represented the results from RUN 5 reported in Li et al. (2019). It was included here for comparison and later discussion. (For interpretation of the references to color in this figure legend, the reader is referred to the web version of this article.)

Table 2
The reduction rate of neck width at a different time in three runs.

RUN 8		RUN 9		RUN 10	
t (h)	R_w (m/h)	t (h)	R_w (m/h)	t (h)	R_w (m/h)
0–11	0.011	0–1	0.0087	0–1	0.102
11–17	0	2–30	0.001	2–22	0.003
17–30	0.009	30–70	0.0004	22–23.33	0.1790
30–35	0.0062	70–89	0.0005		
35–70	0.002	89–101	0.007		
70–72.08	0.728				

to $R_w = 0.0062$ m/h, giving rise to a smaller W_n (i.e., 0.189 m). Further continuous increase of Q to 5.5 m^3/s every 5 h barely changed the value of R_w in the period of 35–70 h, which was about 0.002 m/h, suggesting that the neck under the protection of vegetation gradually approached a dynamic equilibrium, though Q kept increasing. After cutting grass, this quasi-equilibrium was broken, resulting in an abrupt increase of R_w to 0.728 m/h and the occurrence of neck cutoff (Fig. 4).

In RUN 9 with a constant discharge, the first hour of the experiment was controlled by $R_w = 0.0087$ m/h, which led to $W_n = 0.190$ m from the original width of around 0.277 m (Fig. 4). This rate was marginally less than that in RUN 8 during the similar period, indicating that though the initial conditions between experiment runs may not be exactly the same, the initial channel adjustment was similar. In the next period of 2–30 h, R_w remained very low (0.001 m/h), only decreasing W_n by 27.4% (i.e., 0.154 m), demonstrating the resistant effect of vegetation on bank erosion. The subsequently prolonged period was featured by a smaller value of R_w (0.0004 m/h) (Table 2). The R_w value persisted even after the grass was trimmed at the 70th hour and ended at the 89th hour with $W_n = 0.138$ m. Since then, R_w shortly increased to 0.007 m/h and finally triggered neck cutoff at about 101th hour (Fig. 4).

RUN 10 was controlled by variable (near) bankfull discharges starting from 6.86×10^{-3} m^3/s (Fig. 3), which generated a much higher value of R_w (i.e., 0.102 m/h) in the first hour, leading to W_n decreased from the original value of about 0.312 to 0.210 m (Table 2). Although always shaped by (near) bankfull discharges, R_w (i.e., 0.003 m/h) in the period of 2–22 h was slightly higher than that in RUN 9, while lower than that in RUN 8 in a similar period (Fig. 4), causing a relatively slow decrease of W_n to 0.143 m (Table 2). However, the next 1.33 h witnessed a sudden decrease of W_n with $R_w = 0.0099$ m/h. This rate was subsequently increased to 0.1790 m/h, prompting neck cutoff without cutting grass (Fig. 4). Overall, the process of neck reduction was different between runs under variable discharges and that under a constant one.

3.1.2. Bend planform around the neck

In the first stage (i.e., the 0–70 h period) of RUN 8, ripples generally developed on the channel bed and the downstream of bend 3 was eroded considerably at the 30th hour. Yet, the bend planform did not show significant changes until the 50th hour. At the 70th hour, bend 3, 5, and 6 were all enlarged, while deposition dominated the neck near S13 (Fig. 5a and b). Riparian vegetation discernibly changed the flow direction, such that the main flow was diverted to the outer bank of bend 3, and deviated to erode right bank of S13, which reduced the rate of the neck width (Fig. 4). In the second stage (i.e., the 70–84.08 h period), neck cutoff was triggered at the location 0.51 m upstream of S13 and near S22 at $t = 72.08$ h, rather than the expected location (i.e., S13) (Fig. 5c). The main flow was deflected to the right bank of the new cutoff channel, causing enhanced erosion at the inner bank of bend 5 and formation of the submerged bars in the downstream of the cutoff channel (Fig. 5d).

In RUN 9, the neck reduction rate was very low before vegetation was cut at the 70th hour (Fig. 5e and 5f) and neck cutoff happened at the 101.06th hour, about 29 h later than that in RUN 8 (Fig. 5c and g). Additionally, the location of neck cutoff was about 0.14 m upstream of S13, again different from that in RUN 8. Temporal patterns of bend and neck evolution in RUN 10 (Fig. 5i–l) were generally similar to those in RUN 8 and 9 except two distinct characteristics. First, onset of cutoff was much earlier than that in RUN 8 and 9, only taking 21.33 h (Fig. 5k). Second, development of the new cutoff channel was ostentatiously constrained by grass roots in the broken neck, such that the new cutoff channel was obviously narrower than that in RUN 8 and 9 (Fig. 5d, h, and l). These differences showed the combined effect of variable high (near bankfull) discharges and vegetation (lower vegetation density and without grass cutting) on channel morphology in RUN 10 (Table 1).

3.2. Evolution of the new cutoff channel

In all three runs, a new cutoff channel evolved in three phases: (i) creation; (ii) expansion; (iii) stabilization (Fig. 6). From its initial width (W_c) of 0.170 m right after neck cutoff in RUN 8, the new cutoff channel widened at the rate of 10.20 m/h in the first minute and then 0.26 m/h in the first two hours, reaching $W_c = 0.41$ m. In the following 10 h, it experienced brief increase with a much lower rate (i.e. 0.004 m/h) and then remained a stable width of 0.72 m. This width was less than, but comparable to that in both upstream and downstream reaches (i.e., S11 and S24 in Fig. 1a), which was 0.81 and 1.10 m, respectively. Calculation of their width/depth ratio (β) at the end of the experiment showed that $\beta = 13.19$, 13.29, and 16.36 for the new channel, S11, and S24, respectively. The size of the new cutoff channel was similar to that of the upstream reach, but still smaller than that in the downstream reach (Fig. 7a), suggesting that the new cutoff channel was at a near stable stage. Compared with the prolonged period of neck narrowing before grass cutting (i.e., 70th hours) (Fig. 4), it only took less than 5% of this period for the new channel to adjust to this stage.

In RUN 9, the new cutoff channel started with $W_c = 0.182$ m (Fig. 6), followed by a swift increase at the rate of 10.92 m/h in the first minute and a reduced one of 0.33 m/h in the following two hours. Consequently, the channel width increased more than four times, resulting in $W_c = 0.838$ m. In the period of 2–12 h, the increasing rate of W_c was quickly reduced to 0.025 m/h, resulting in $W_c = 1.088$ m at the end of the period. This width kept unchanged in the rest of the hours (Fig. 6) and was greater than that in S11 and S26, which was 0.976 and 0.844 m, respectively. The β value, which was 22.57, was similar to that at S11 (i.e., 23.13), but greater than that at S26 (i.e., 14.83) (Fig. 7b). Apparently, the new channel had reached a new equilibrium condition within a very

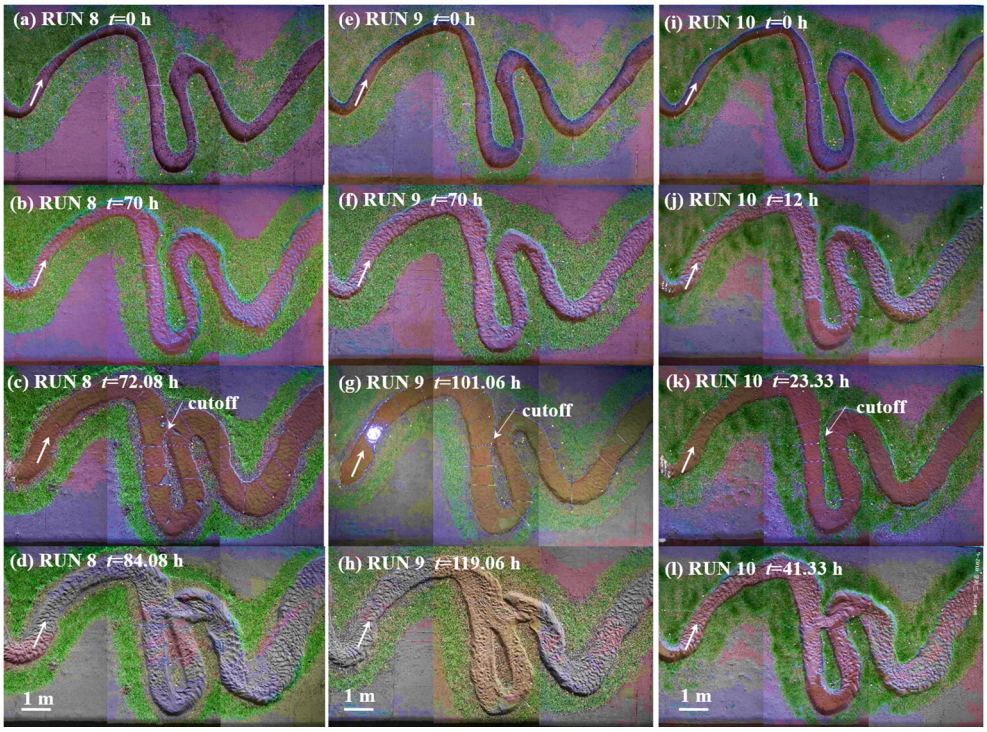

Fig. 5. Temporal changes of bend planform around the neck (bend 3–6) from the initial morphology to cutoff occurrence in RUN 8, 9, and 10.

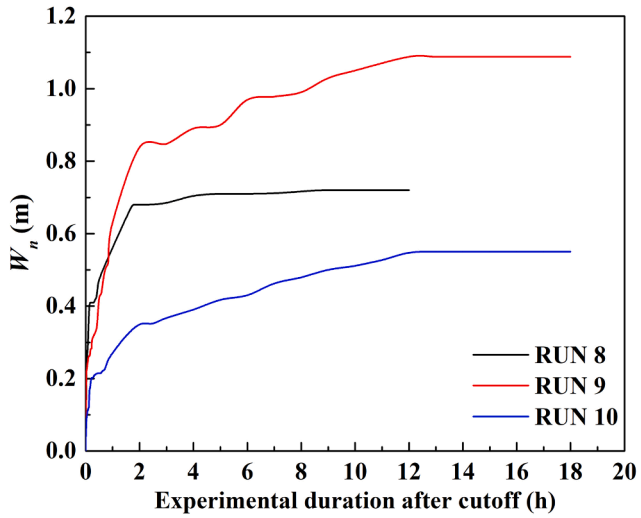

Fig. 6. Width changes of the new cutoff channel in the post-cutoff period in RUN 8, 9, and 10.

short time period, which was only less than 15% of the period of neck narrowing before cutting grass (Fig. 4).

The cutoff channel in RUN 10 began with $W_c = 0.063$ m after cutoff and promptly increased to 0.19 m within about 40 min (Fig. 6). In the next one hour, W_c increased to 0.270 m with a reduced increasing rate of 0.27 m/h. From 1.33 to 12th hour, the increasing rate was further reduced to 0.0198 m/h, giving rise to $W_c = 0.550$ m. This width hardly changed in the rest of time (Fig. 6). Yet, it was much less than that at S11 and S26, which was 0.987 and 0.961 m, respectively, suggesting that the new channel still needs time to reach a new equilibrium condition. Similarly, the new channel had $\beta = 16.57$ and was clearly less than that in S16 and S27, which was 21.73 and 20.33, respectively (Fig. 7c). This difference again indicated that the new channel had not reached a new equilibrium condition yet, though its adjustment had already taken about 50% of the time for the occurrence of neck cutoff (Fig. 4) and input discharges were relatively high (Fig. 3). Responses of channel morphology to variable discharges (i.e., RUN 8 and 10) were different from those to constant ones (i.e., RUN 9). The former took longer time to reach a stable condition (Fig. 6) and the higher discharge in RUN 8 after cutoff than that in RUN 10 tended to enhance bank erosion more than to increase bed incision (Fig. 7).

3.3. Impact of neck cutoff on channel morphodynamics

3.3.1. Slope adjustment

Adjustment of channel slopes was characterized by temporal trends of the slopes in the upstream (S_u) and downstream (S_d) reach (i.e., the slopes of the S7-S13 and S21-S30 sections in Fig. 1). Although RUN 8 had variable (increasing) discharges, while RUN 9 had a constant discharge (Fig. 3), their upstream reaches followed a similar temporal trend in the first 70 h: decreasing slightly during the early period and then remained nearly constant (Fig. 8a). In RUN 10, S_u increased in the first 15 h, though the discharge decreased drastically. Then, it followed a similar trend to those in RUN 8 and 9 before the 70th hour. Cutting grass in RUN 8 triggered cutoff shortly, while still allowed the neck to survive for about 30 h before cutoff (Fig. 8a) showing the much stronger impact of the variable (increasing) discharges on bank erosion than the constant one. Cutoff caused a sharp decrease of S_u in RUN 8 and 10 with variable discharges (regardless of the pattern of variability), but increase of S_u for a few hours before decreasing. The reduction of S_u in all runs could be related to the possible backwater effect from the oxbow segment because the original new cutoff channel was very small. It also indicated that the bed of the upstream reach in RUN 8 and 10 with variable discharges did not experience discernable incision.

In the downstream reach, S_d initially decreased in the early period of all three runs and then oscillated before cutoff (Fig. 8a). Different from the upstream reach where S_u was the lowest in RUN 10, the downstream reach showed the lowest S_d in RUN 8. After cutting grass, S_d in RUN 9 remained the oscillating pattern rather than gradually decreasing as shown in the upstream reach. The more striking distinction between the

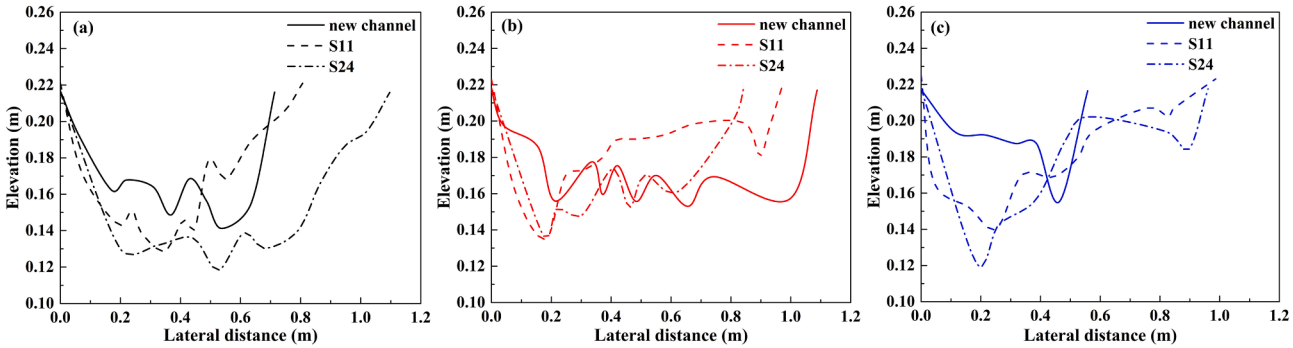

Fig. 7. Morphology of the representative cross sections in the three reaches of the meandering channel at the end of RUN 8, 9, and 10 (the zero on the horizontal axis represents the left bank).

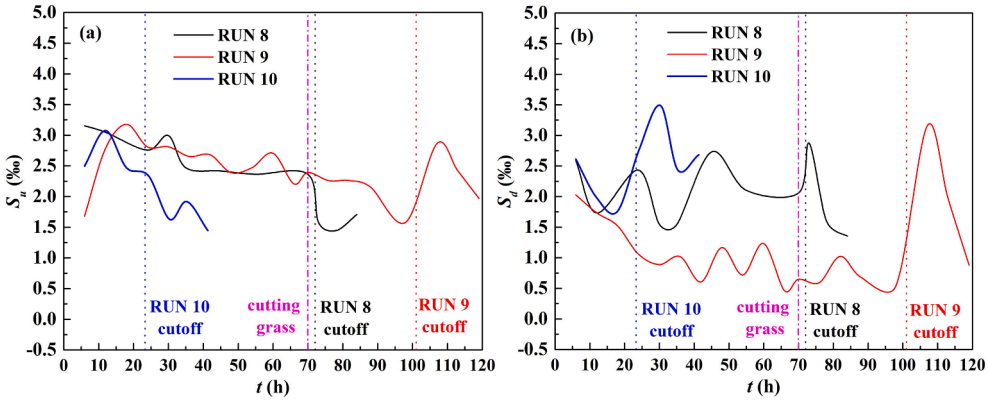

Fig. 8. Temporal changes of S_u and S_d in the three experiments. The red vertical line represented the moment when grass was trimmed, while the black vertical dot dash line denoted the moment when neck cutoff occurred. (a) RUN 8, (b) RUN 9, and (c) RUN 10. (For interpretation of the references to color in this figure legend, the reader is referred to the web version of this article.)

two reaches was attested by the swift increase of S_d immediately after cutoff in all three experiments (Fig. 8b). This increase was mainly caused by the raised water level at the convergence of the new channel and the upper end of the downstream channel. However, it is important to note that the increase of water level was not caused by suddenly increased sediment supply from the new channel as typically happened after chute cutoff (Zinger et al., 2011). The neck cutoff was initiated by gradually enhanced seepage flow, which first induced visible surface flow on top of the very narrow neck, e.g., less than 0.15 m wide in RUN 10 (Fig. 4). Then, the surface flow became larger and larger due to the gradually lowered elevation of the neck top, which was caused by increased erosion. As such, sediment supply to the downstream reach was limited due to vegetation inhibiting bank erosion, but water level was increased quickly due to shortened flow path. This mechanism only exists during the development of the new channel, which is short. After the new channel gained its main shape within two hours following cutoff (Fig. 6), the raised water level began to subside leading to the decrease of S_d (Fig. 8b). The above-mentioned mechanism explained why S_d increased promptly and then decreased quickly as compared with the changes of S_u in all three runs.

3.3.2. *Adjustment of cross sections*

In the cross section within the upstream reach (i.e., S11), β increased with time in all three runs with its magnitudes arranged in the order of

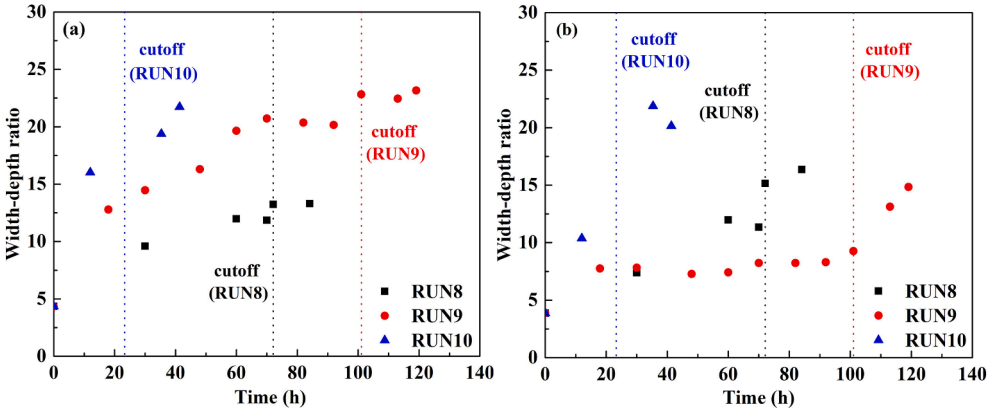

Fig. 9. Temporal changes of the width-depth ratio in the representative cross sections of the upstream (a) and downstream (b) reaches in three experiments.

RUN 10, 9, and 8 (Fig. 9a). However, β values in RUN 9 were generally higher than those in RUN 8 (Fig. 9a), though RUN 9 had lower discharges than RUN 8 (Fig. 3). This apparent contradiction might be reconciled by the fact that in RUN 9, riparian vegetation had relatively less density, which allowed the banks easier to be eroded, reflecting the coupled effect of vegetation and discharges on channel adjustment. The higher degree of channel widening in RUN 10 suggested that the impact of input discharges was higher than that of vegetation. In the downstream reach, while β still increased with time in all runs, the patterns were different from those in the upstream reach in three ways. First, β in RUN 9 was larger than that in RUN 8, indicating more downstream erosion happened in the former. Second, cutoff caused discernable higher degrees of increase in β for all three experiments (Fig. 9b), suggesting that cutoff has enhanced channel incision and bank erosion in the downstream reach. This result is consistent with the mechanism of neck cutoff described in Section 3.3.1. Third, the rate of increase in β for RUN 10 was significantly higher than those for RUN 8 and 9. Inasmuch as the ratio of the maximum stream power between RUN 10 and 8 was only 0.87 (see Figs. 3 and 8b). This higher increase rate of β in RUN 10 cannot be attributed to its discharges as after cutoff, discharges in RUN 10 were indeed lower than those in RUN 8 (Fig. 3). The only plausible interpretation connects to the role of vegetation as RUN 10 had lower density of vegetation cover than RUN 8 (Table 1).

4. Discussions

4.1. Effect of riparian vegetation on neck cutoff

To our knowledge, our flume experiments are the first set of such that successfully achieved neck cutoff in a highly sinuous meandering channel, whose banks and floodplain are covered by vegetation. Thus, the role of vegetation in the process of bend evolution toward neck cutoff may be revealed by examining comparable pairs of experimental runs. If the degree of vegetation coverage around the meandering channel is defined as $\Delta = L_s / L_r$ where L_s and L_r are mean stem length and mean root length, respectively, then for RUN 5 without seeding grass reported in Li et al. (2019), $\Delta = 0$, while for RUN 10, $\Delta = 1.08$. Their temporal trends of neck reduction up to the occurrence of cutoff may be reasonably well described by an empirical equation (Fig. 10):

$$\frac{b}{w} = \left[\frac{1}{m} ln\left(\frac{T_t - T_0}{t - T_0}\right)\right]^{\frac{5}{2}} \quad (1)$$

where T_0 is the reference time when the neck width (b) is close to the mean channel width (w), T_t is the time when neck cutoff happens (i.e., $b = 0$), t is the time between T_0 and T_t, and m is a constant controlling the general gradient of the curve. Based on eq. (1), at $t = 0$, the dimensionless neck width (i.e., b/w) for the two experiments was about the same, which was 0.22. Then, RUN 5 took 19 h, while RUN 10 would last 29 h for the occurrence of neck cutoff, but its higher discharges (see Fig. 4) accelerated this evolution process (Fig. 10). Even with the much higher discharges in RUN 10, existence of vegetation in the banks significantly delays the reduction of neck width by enhancing bank resistance. Similarly, for RUN 5 and 9 that had similar constant discharges, but difference vegetation coverage (i.e., $\Delta = 0$ and 1.15, respectively), it took about 15 h in RUN 5, while about 90 h in RUN 9 to initiate neck cutoff from the time when they had similar neck width ($b =$ 0.18 m) (Fig. 4). Although vegetation cover in RUN 8 (i.e., $\Delta = 1.75$), was higher than that (i.e., $\Delta = 1.15$) in RUN 9, the rate of neck reduction, which is represented by the slope of the curve in Fig. 4, was much higher in the former than that in the latter. This higher rate must be related to the higher discharges in RUN 8 than in RUN 9. The even higher discharges in RUN 10 triggered neck cutoff in a much short time period than RUN 8 and 9. These results indicate that the magnitude of flow also affects the evolution process of a bend toward neck cutoff.

Our experimental results showed the strong effect of vegetation on reducing the degree of bank erosion, such that neck cutoff would not happen in RUN 9 without trimming vegetation. In natural rivers, this hindering effect supports the fact of less neck cutoffs than chute cutoffs (Camporeale et al., 2005; Howard, 1992; Sun et al., 1996). More specifically, vegetation in natural rivers could extend the evolution period after the neck width reduces to the mean channel width, as shown in Fig. 10. Unfortunately, previous studies on neck cutoffs in natural rivers did not have such information for us to compare our results with it. Future studies are needed to fill this gap.

4.2. Channel adjustment after neck cutoff

Lateral migration rates (M_c) of the upstream and downstream reaches were represented by the change of the channel centerline per unit time at S7-S13 and S21-S26, respectively. In all three runs, M_c increased more significantly in the downstream reach than that in the upstream reach (Fig. 11), indicating the generally higher impact of cutoff on lateral migration of the downstream channel. The effect of vegetation on channel adjustment was clearly demonstrated in the downstream reach where the migration rate in RUN 9 with no vegetation coverage was higher than that in RUN 10 with vegetation, though the latter had much higher discharges. The even higher M_c in RUN 8 for both the upstream and downstream reaches reflected that the driving of channel adjustment by higher discharges overweighs the resistance to the changes of channel morphology provided by vegetation on channel banks.

Many studies have revealed that chute cutoff in natural rivers is typically accompanied with rapid incision of the cutoff channel that leads to sudden increase of downstream sediment flux (Fuller et al., 2003; Zinger et al., 2011, 2013). This change can create sediment pulses in the downstream channel that are responsible for the accelerated lateral migration, bend widening, and cutoff clustering (Ielpi et al., 2021; Schwenk and Foufoula-Georgiou, 2016; Viero et al., 2018). Based on the findings from our flume experiments on neck cutoff, we argue

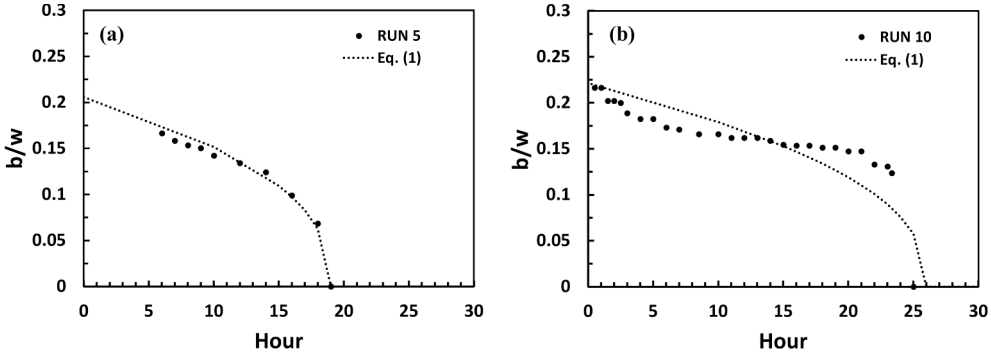

Fig. 10. Temporal changes of neck widths over the experimental periods and the empirically fitted curve. (a) RUN 5 reported in Li et al. (2019); (b) RUN 10 in this study.

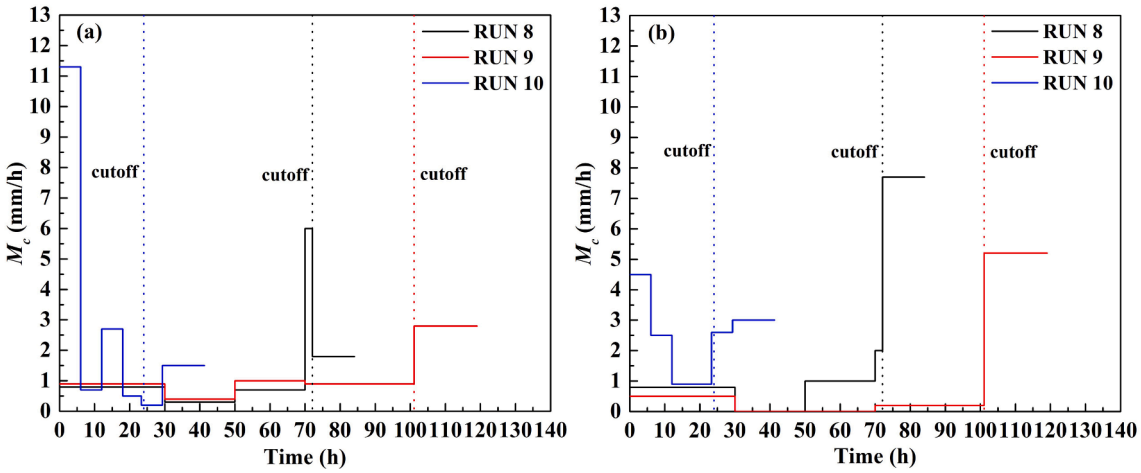

Fig. 11. Lateral migration rates of the upstream (a) and downstream reaches in the three experiments.

that morphological responses of the downstream channels to both neck and chute cutoffs are similar, but via different mechanisms. The former are mainly caused by increased hydraulics (i.e., slopes), while the latter are induced by changed bedforms due to bed deposition from augmented sediment supply. It follows that the geomorphological differences between neck and chute cutoffs lie in their different time scales at which the planform morphology of meandering rivers is disturbed.

4.3. Limitations and significance of our flume experiments

We realized that interpretation of our experimental results should be constrained by some limitations in our experimental design. First, the meandering channel created in the flume was designed based on geometric similarity rather than hydraulic and sediment similarity (Li et al., 2019). The latter requires a channel with greater depths and lightweight plastic sediment (Braudrick et al., 2009), which cannot be physically achieved in the existing laboratory facility. Consequently, time periods describing processes of neck cutoff in all experiments could not be temporally scaled to those of natural neck cutoffs. Second, materials molding the laboratory channel were sand grains with a uniform size. They failed to represent the cohesive banks and bi-mode bed materials (i.e., gravels and sand/silt) in real meanders. Thus, hydraulic variables during these experiments may not reflect the true hydrodynamic conditions for neck cutoff in natural meandering rivers. Third, detailed impact of grass heights and density on channel flows was not quantified as our focus was on their lumped effect. Despite of these limitations, our experiments provided unique and valuable insight into impact of riparian vegetation and variable discharges on neck cutoff.

Thus far, experimental studies have focused on the role of vegetation in changing flow hydrodynamics, affecting morphological changes of braided channels, or maintaining banks of meandering channels (Braudrick et al., 2009; Elliott et al., 2019; Kui et al., 2019; Kyuka et al., 2021; Simon and Collison, 2002; Tal and Paola, 2010; Yang et al., 2018). It is well known that neck cutoff in natural meandering rivers is extremely difficult to be observed due to its slow development and sudden occurrence. Riparian vegetation has played a critical role in extending the evolution period of neck cutoff. As such, processes of meander cutoff could only be indirectly examined in terms of remote sensing imagery (Constantine and Dunne, 2008; Li et al., 2017; Schwenk et al., 2015; Schwenk and Foufoula-Georgiou, 2016; Viero et al., 2018) and depicted using a conceptual three-stage model (Richards and Konsoer, 2020). Our experiments provide a new way of reproducing processes of neck cutoff in laboratory flumes for better understanding processes controlling development of neck cutoff.

5. Conclusions

In this study, we performed three flume experiments (i.e., RUN 8, 9, and 10) in a highly convoluted meandering channel whose banks and floodplain were covered by riparian vegetation (i.e., *Festuca elata*). These experiments had different input discharges and vegetation. Results from them provided new insight into processes and mechanism during and after neck cutoff.

Vegetation significantly reduces the neck narrowing rate regardless of magnitudes and patterns of input discharges, suggesting that bank erosion around the bend neck of highly sinuous meandering rivers in the Zoige basin (and other alluvial environments with vegetation cover) has been effectively constrained by soil-vegetation mixture, such that neck cutoff often takes much longer time to occur than it appears. This also infers that neck cutoff in natural meandering rivers may be more induced by the second mode as the first mode requires high flows with low probability of occurrence. In all experiments, occurrence of neck cutoff was started by reduction of elevation on top of the narrowest neck due to enhanced seepage flow, suggesting that initiation of neck cutoff in the final moment is not due to bank erosion, but seepage force (Han et al., 2015; Li et al., 2019). Understanding this mechanism is extremely important as it provides a means of inferring when the prolonged trend of neck narrowing may be terminated.

The new cutoff channel evolves quickly to the size similar to those upstream and downstream, suggesting that meandering rivers can recover quickly from neck cutoff. The impact of neck cutoff on the downstream reach is more significant than on the upstream one. More importantly, the downstream channel adjustments (e.g., widening and increased lateral migration) due to neck cutoff are similar to those caused by chute cutoff. This similarity suggests that geomorphological distinction of the impact on meandering rivers between neck and chute cutoffs should be reflected in the different temporal scales at which they interrupt evolution process of these rivers.

Declaration of Competing Interest

The authors declare the following financial interests/personal relationships which may be considered as potential competing interests: Zhiwei Li reports financial support was provided by National Natural Science Foundation of China. Zhiwei Li reports financial support was provided by Science & Technology Department of Hunan Province of China. Zhiwei Li reports financial support was provided by Natural Science Foundation of Hubei Province of China. Peng Gao reports a relationship with Syracuse University that includes: employment. Xinyu Wu reports a relationship with Changsha University of Science & Technology that includes: employment.

Acknowledgements

This study was supported by the National Natural Science Foundation of China (51979012, U2040215), Fundamental Research Funds for the Central Universities (2042021kf0199), Natural Science Foundation of Hubei Province of China (2020CFB554), and Major Project of Hunan Science & Technology Plan of China (2018SK1010). We appreciate Prof. Xuyue Hu for the support of constructing the flume, and Dr. Ielpi and an anonymous reviewer for insightful comments and suggestions.

References

Braudrick, C.A., Dietrich, W.E., Leverich, G.T., Sklar, L.S., 2009. Experimental evidence for the conditions necessary to sustain meandering in coarse-bedded rivers. Proc. Nat. Acad. Sci. 106 (40), 16936–16941.

Camporeale, C., Perona, P., Porporato, A., Ridolfi, L., 2005. On the long-term behavior of meandering rivers. Water Resour. Res. 41 (W12403) https://doi.org/10.1029/2005wr004109.

Camporeale, C., Perucca, E., Ridolfi, L., 2008. Significance of cutoff in meandering river dynamics. J. Geophys. Res. 113 (F01001). https://10.1029/2006jf000694.

Camporeale, C., Perucca, E., Ridolfi, L., Gurnell, A.M., 2013. Modeling the interactions between river morphodynamics and riparian vegetation. Reviews of Geophys. 51 (3), 379–414.

Camporeale, C., Ridolfi, L., 2010. Interplay among river meandering, discharge stochasticity and riparian vegetation. J. Hydrol. 382 (1-4), 138–144.

Constantine, J.A., Dunne, T., 2008. Meander cutoff and the controls on the production of oxbow lakes. Geology 36 (1), 23. https://doi.org/10.1130/G24130A.110.1130/2008009.

Coomes, O.T., Abizaid, C., Lapointe, M., 2009. Human modification of a large meandering Amazonian River: genesis, ecological and economic consequences of the Masisea cutoff on the central Ucayali. Peru. AMBIO: A J. Human Envir. 38 (3), 130–134.

Crosato, A., Saleh, M.S., 2011. Numerical study on the effects of floodplain vegetation on river planform style. Earth Surf. Process. Landf. 36 (6), 711–720.

Dehsorkhi, E.N., Afshar, S., Sui, J., 2010. Effects of vegetation channel banks and gravel size on flow structure. Inter. J. Sediment Res. 25 (2), 110–118.

Edmaier, K., Burlando, P., Perona, P., 2011. Mechanisms of vegetation uprooting by flow in alluvial non-cohesive sediment. Hydrol. Earth Sys. Sci. 15 (5), 1615–1627.

Eekhout, J.P.C., Hoitink, A.J.F., 2015. Chute cutoff as a morphological response to stream reconstruction: the possible role of backwater. Water Resour. Res. 51 (5), 3339–3352.

Elliott, S.H., Tullos, D.D., Walter, C., 2019. Physical modeling of the feedbacks between a patch of flexible Reed Canarygrass (Phalaris arundinacea), wake hydraulics, and downstream deposition. Envir. Fluid Mech. 19 (1), 255–277.

Erskine, W., McFadden, C., Bishop, P., 1992. Alluvial cutoffs as indicators of former channel conditions. Earth Surf. Process. Landf. 17 (1), 23–37.

Fares, Y.R., 2000. Changes of bed topography in meandering rivers at a neck cutoff intersection. J. Envir. Hydrol. 8, 1–18.

Fuller, I.C., Large, A.R.G., Milan, D.J., 2003. Quantifying channel development and sediment transfer following chute cutoff in a wandering gravel-bed river. Geomorphology 54 (3-4), 307–323.

Gao, P., Li, Z., Yang, H., 2021. Variable discharge control composite bank erosion in Zoige meandering rivers. Catena 204, 105384.

Gay, G.R., Gay, H.H., Gay, W.H., Martinson, H.A., Meade, R.H., Moody, J.A., 1998. Evolution of cutoffs across meander necks in Powder River, Montana, USA. Earth Surf. Process. Landf. 23 (7), 651–662.

Goodson, J.M., Gurnell, A.M., Angold, P.G., Morrissey, I.P., 2016. Riparian seed banks: structure, process and implications for riparian management. Progr. Phys. Geogra. 25, 301–325.

Gran, K., Paola, C., 2001. Riparian vegetation controls on braided stream dynamics. Water Resour. Res. 37 (12), 3275–3283.

Güneralp, İ., Marston, R.A., 2012. Process–form linkages in meander morphodynamics: Bridging theoretical modeling and real world complexity. Progr. Phys. Geogra. 36 (6), 718–746.

Guo, X., Chen, D., Parker, G., 2019. Flow directionality of pristine meandering rivers is embedded in the skewing of high-amplitude bends and neck cutoffs. Proc. Nat. Acad. Sci. 116 (47), 23448–23454.

Han, B., Chu, H.-H., Endreny, T.A., 2015. Streambed and water profile response to in-channel restoration structures in a laboratory meandering stream. Water Resour. Res. 51 (11), 9312–9324.

Hooke, J.M., 1995. River channel adjustment to meander cutoffs on the River Bollin and River Dane, northwest England. Geomorphology 14 (3), 235–253.

Hooke, J.M., 2004. Cutoffs galore!: occurrence and causes of multiple cutoffs on a meandering river. Geomorphology 61 (3-4), 225–238.

Hooke, J.M., 2013. River meandering. In: Shroder J. (Editor in Chief) Wohl E. (Ed.), Treatise on Geomorphology. Academic Press, San Diego, CA, vol. 9, Fluvial Geomorphology, pp. 260–288.

Hopkinson, L., Wynn, T., 2009. Vegetation impacts on near bank flow. Ecohydrol. 2 (4), 404–418.

Howard, A.D., 1992. Modeling channel migration and floodplain sedimentation in meandering streams. In: Carling, P.A., Petts, G.E. (Eds.), Lowland Floodplain Rivers: Geomorphological Perspectives. John Wiley & Sons Ltd., Chichester, UK, pp. 1–41.

Ielpi, A., Lapotre, M.G.A., 2020. A tenfold slowdown in river meander migration driven by plant life. Nat. Geosci. 13 (1), 82–86.

Ielpi, A., Lapôtre, M.G.A., Finotello, A., Ghinassi, M., 2021. Planform-asymmetry and backwater effects on river-cutoff kinematics and clustering. Earth Surf. Process. Landf. 46 (2), 357–370.

Krzeminska, D., Kerkhof, T., Skaalsveen, K., Stolte, J., 2019. Effect of riparian vegetation on stream bank stability in small agricultural catchments. Catena 172, 87–96.

Kui, L.i., Stella, J.C., Diehl, R.M., Wilcox, A.C., Lightbody, A., Sklar, L.S., 2019. Can environmental flows moderate riparian invasions? The influence of seedling morphology and density on scour losses in experimental floods. Freshwater Biol. 64 (3), 474–484.

Kyuka, T., Yamaguchi, S., Inoue, Y., Arnez Ferrel, K.R., Kon, H., Shimizu, Y., 2021. Morphodynamic effects of vegetation life stage on experimental meandering channels. Earth Surf. Process. Landf. 46 (7), 1225–1237.

Lewis, G.W., Lewin, J., 1983. Alluvial cutoffs in Wales and the Borderlands. In: Collinson, J.D., Lewin, J. (Eds.), Modern and Ancient Fluvial Systems. Blackwell, Oxford, pp. 145–154.

Li, Z., Gao, P., 2019. Channel adjustment after artificial neck cutoffs in a meandering river of the Zoige basin within the Qinghai-Tibet Plateau, China. Catena 172, 255–265.

Li, Z., Wu, X., Gao, P., 2019. Experimental study on the process of neck cutoff and channel adjustment in a highly sinuous meander under constant discharges. Geomorphology 327, 215–229.

Li, Z.W., Yu, G.A., Brierley, G., Wang, Z.Y., 2016. Vegetative impacts upon bedload transport capacity and channel stability for differing alluvial planforms in the Yellow River source zone. Hydrol. Earth Sys. Sci. 20 (7), 3013–3025.

Li, Z., Yu, G.-A., Brierley, G.J., Wang, Z., Jia, Y., 2017. Migration and cutoff of meanders in the hyperarid environment of the middle Tarim River, northwestern China. Geomorphology 276, 116–124.

Liu, J., Li, Z., Tian, S., Liu, C., 2017. Study on meander cutoffs of the Lower Weihe River in recent 60 years. J. Sediment Res. 42, 12–19 (English abstract in Chinese).

Lonsdale, P., Hollister, C.D., 1979. Cut-offs at an abyssal meander south of Iceland. Geology 7 (12), 597. https://doi.org/10.1130/0091-7613(1979)7<597:CAAAMS>2.0.CO;2.

Midgley, T.L., Fox, G.A., Heeren, D.M., 2012. Evaluation of the bank stability and toe erosion model (BSTEM) for predicting lateral retreat on composite streambanks. Geomorphology 145-146, 107–114.

Nepf, H.M., 2012. Flow and transport in regions with aquatic vegetation. Ann. Rev. Fluid Mech. 44 (1), 123–142.

Ondruch, J., Máčka, Z., Šulc Michalková, M., Putiška, R., Knot, M., Holík, P., Mířijovský, J., Jenčo, M., 2018. Response of channel dynamics to recent meander neck cut-off in a lowland meandering river with artificial training history: the Morava River, Czech Republic. Hydrol. Sci. J. 63 (8), 1236–1254.

Oorschot, M.V., Kleinhans, M., Geerling, G., Middelkoop, H., 2016. Distinct patterns of interaction between vegetation and morphodynamics. Earth Surf. Process. Landf. 41 (6), 791–808.

Pan, C.S., Shi, S.C., Duan, W.Z., 1978. A study of the channel development after the completion of artificial cutoffs in the middle Yangtze River. Scientia Sinica 21, 783–804.

Perucca, E., Camporeale, C., Ridolfi, L., 2007. Significance of the riparian vegetation dynamics on meandering river morphodynamics. Water Resour. Res. 43 (W03430) https://doi.org/10.1029/2006WR005234.

Pollen-Bankhead, N., Simon, A., 2010. Hydrologic and hydraulic effects of riparian root networks on streambank stability: is mechanical root-reinforcement the whole story? Geomorphology 116 (3-4), 353–362.

Richards, D., Konsoer, K., 2020. Morphologic adjustments of actively evolving highly curved neck cutoffs. Earth Surf. Process. Landf. 45 (4), 1067–1081.

Schwendel, A.C., Nicholas, A.P., Aalto, R.E., Sambrook Smith, G.H., Buckley, S., 2015. Interaction between meander dynamics and floodplain heterogeneity in a large tropical sand-bed river: the Rio Beni. Bolivian Amazon. Earth Surf. Process. Landf. 40 (15), 2026–2040.

Schwenk, J., Foufoula-Georgiou, E., 2016. Meander cutoffs nonlocally accelerate upstream and downstream migration and channel widening. Geophys. Res. Letters 43, 1–10. https://doi.org/10.1002/2016GL071670.

Schwenk, J., Lanzoni, S., Foufoula-Georgiou, E., 2015. The life of a meander bend: Connecting shape and dynamics via analysis of a numerical model. J. Geophys. Res. Earth Surf. 120 (4), 690–710.

Seminara, G., 2006. Meanders. J. Fluid Mech. 554 (-1), 271. https://doi.org/10.1017/S0022112006008925.

Simon, A., Collison, A.J.C., 2002. Quantifying the mechanical and hydrologic effects of riparian vegetation on streambank stability. Earth Surf. Process. Landf. 27 (5), 527–546.

Słowik, M., 2016. The influence of meander bend evolution on the formation of multiple cutoffs: findings inferred from floodplain architecture and bend geometry. Earth Surf. Process. Landf. 41, 626–641.

Stølum, H.H., 1996. River meandering as a self-organisation process. Science 271, 1710–1713.

Sun, T., Meakin, P., Jøssang, T., Schwarz, K., 1996. A simulation model for meandering rivers. Water Resour. Res. 32 (9), 2937–2954.

Tal, M., Paola, C., 2007. Dynamic single-thread channels maintained by the interaction of flow and vegetation. Geology 35 (4), 347. https://doi.org/10.1130/G23260A.110.1130/2007083.

Tal, M., Paola, C., 2010. Effects of vegetation on channel morphodynamics: results and insights from laboratory experiments. Earth Surf. Process. Landf. 35 (9), 1014–1028.

van Dijk, W.M., Schuurman, F., van de Lageweg, W.I., Kleinhans, M.G., 2014. Bifurcation instability and chute cutoff development in meandering gravel-bed rivers. Geomorphology 213, 277–291.
van Dijk, W.M., Teske, R., van de Lageweg, W.I., Kleinhans, M.G., 2013. Effects of vegetation distribution on experimental river channel dynamics. Water Resour. Res. 49 (11), 7558–7574.
van Dijk, W.M., van de Lageweg, W.I., Kleinhans, M.G., 2012. Experimental meandering river with chute cutoffs. J. Geophys. Res. Earth Surf. 117 (F03023) https://doi.org/10.1029/2011JF002314.
Viero, D.P., Dubon, S.L., Lanzoni, S., 2018. Chute cutoffs in meandering rivers: formative mechanisms and hydrodynamic forcing, International Association of Sedimentologists. IAS Special Publications.
Wang, Z., Li, Z., Xu, M., Yu, G., 2016. River Morphodynamics and Stream Ecology of the Qinghai-Tibet Plateau. CRC Press, Taylor & Francis Ltd, Netherland.
Winkley, B.R., 1977. Man-made cutoffs on the lower Mississippi River, conception, construction, and river response. Vicksburg, Mississippi.
Yang, S., Bai, Y., Xu, H., 2018. Experimental analysis of river evolution with riparian vegetation. Water 10 (11), 1500. https://doi.org/10.3390/w10111500.
Yin, X., 1965. Preliminary experiment study on formation and evolution of meandering river. Acta Geogra. Sinica 31, 287–303.
Zhu, H., Gao, P., Li, Z., Fu, J., Li, G., Liu, Y., Li, X., Hu, X., 2020. Impacts of degraded alpine swamp meadow on tensile strength of river bank: a case study of the Upper Yellow River. Water 12, 2348.
Zinger, J.A., Rhoads, B.L., Best, J.L., 2011. Extreme sediment pulses generated by bend cutoffs along a large meandering river. Nat. Geosci. 4 (10), 675–678.
Zinger, J.A., Rhoads, B.L., Best, J.L., Johnson, K.K., 2013. Flow structure and channel morphodynamics of meander bend chute cutoffs: a case study of the Wabash River, USA. J. Geophys. Res. Earth Surf. 118 (4), 2468–2487.